Electromagnetics

ISSN: 0272-6343 (Print) 1532-527X (Online) Journal homepage: http://www.tandfonline.com/loi/uemg20

Design of Single-Layer Microstrip Antennas for Dual-Frequency-Band Ratio Adjustment with Circular Polarization Characteristics

Taekki Lee, Hosung Choo, Byung-Jun Jang & Gangil Byun

To cite this article: Taekki Lee, Hosung Choo, Byung-Jun Jang & Gangil Byun (2017) Design of Single-Layer Microstrip Antennas for Dual-Frequency-Band Ratio Adjustment with Circular Polarization Characteristics, Electromagnetics, 37:4, 224-232, DOI: 10.1080/02726343.2017.1316231

To link to this article: http://dx.doi.org/10.1080/02726343.2017.1316231

Published online: 09 May 2017.

ELECTROMAGNETICS
2017, VOL. 37, NO. 4, 224–232
http://dx.doi.org/10.1080/02726343.2017.1316231

Design of Single-Layer Microstrip Antennas for Dual-Frequency-Band Ratio Adjustment with Circular Polarization Characteristics

Taekki Lee[a], Hosung Choo[b], Byung-Jun Jang[c] and Gangil Byun[d]

[a]The 1st R & D Institute, Agency for Defense Development, Daejeon, Korea; [b]School of Electronic and Electrical Engineering, Hongik University, Seoul, Korea; [c]School of Electronics Engineering, Kookmin University, Seoul, Korea; [d]Research Institute of Science and Technology, Hongik University, Seoul, Korea

ABSTRACT

This article proposes the design of a single-layer circular polarization antenna for flexible dual-frequency-band ratio adjustment. The antenna consists of an inner circular patch and an outer ring patch that is electromagnetically coupled to the circular patch. The circular patch is fed by two ports of a hybrid chip coupler, and the dual-frequency-band ratio is adjusted by varying the gap distance between the two patches. For verification, the proposed antenna was fabricated to measure its antenna characteristics in a full anechoic chamber, and the results demonstrated that the antenna is suitable for flexible adjustment of the dual-frequency-band ratio from 1.24 to 1.8, with an average axial ratio of 2.4 dB.

ARTICLE HISTORY
Received 24 November 2016
Accepted 16 March 2017

KEYWORDS
Dual-band CP antenna; dual-frequency-band ratio adjustment; microstrip antenna

1. Introduction

Dual-band antennas have been widely used in wireless communications systems to achieve more flexible frequency coverage, multi-functionality, and frequency diversity (Zhang et al., 2014; Reddy et al., 2014). These advantages become more effective for satellite signal reception, such as Global Positioning Systems (GPSs) and Sirius XM satellite radio, when the antennas have dual-band circular polarization (CP) characteristics (Ta & Park, 2014; Nasimuddin et al., 2010; Bao & Ammann, 2007). Thus, much effort has been expended to develop dual-band CP antennas; however, most previous studies were focused on achieving dual resonances for fixed frequency points (Smolders et al., 2013; Byun et al., 2015; Hsieh et al., 2012; Cai et al., 2015). In addition, the tuning capability of their frequency points has been difficult to achieve because they were often limited to a multi-layer structure to stack multiple resonating patches (Byun et al., 2014; Falade et al., 2013; Edimo et al., 1994). Although the ratio between two resonant frequencies, denoted as the dual-frequency-band ratio, can be adjusted by applying the reconfigurable antenna structure, as described in (Abutarboush et al., 2012; Nor et al., 2013; Hung & Chiu, 2015; Behdad & Sarabanni, 2006; Hu et al., 2009), the focus of these studies has mainly been on switching the resonant frequencies without an in-depth consideration of flexible adjustment for the dual-frequency-band ratio.

CONTACT Gangil Byun kylebyun@gmail.com Research Institute of Science and Technology, Hongik University, 94 Wausan-ro, Mapo-gu, Seoul 04066, Korea.

Color versions of one or more of the figures in the article can be found online at www.tandfonline.com/uemg

In this article, we propose the design of a dual-band CP antenna with a single-layer structure for flexible dual-frequency-band ratio adjustment. The proposed antenna consists of an inner circular patch and an outer ring patch, which are separated by a gap in the same layer, and the dual-frequency-band ratio is adjusted by simply varying the gap. The circular patch is fed by two ports of a hybrid chip coupler placed at the bottom of the ground, which is employed to provide a flexible dual-frequency-band ratio adjustment with a broad CP bandwidth. The ring patch is then electromagnetically coupled to the circular patch as excitation, and the coupling strength is adjusted by varying the gap and the substrate height. To demonstrate the capability of the dual-frequency-band ratio adjustment, the proposed antenna was applied for the GPS L1 and L2 bands, and the antenna was fabricated to measure its radiation characteristics in a full anechoic chamber. We verified that the dual-frequency-band ratio can be adjusted from 1.24 to 1.8 by varying the gap distance without degradation of the impedance matching and CP properties.

2. Design approach and proposed antenna

Figure 1 shows the geometry of the proposed antenna for the flexible dual-frequency-band ratio adjustment. The proposed antenna consists of an inner circular patch and an outer

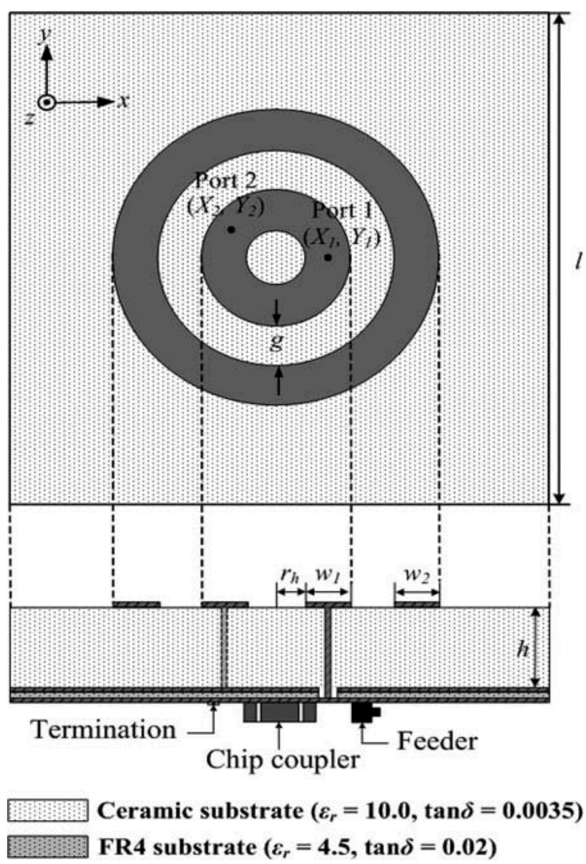

Figure 1. Geometry of the proposed antenna.

ring patch that are printed on a dielectric substrate having a height of h. The circular patch has a radius of $r_h + w_1$, which is designed to be about a quarter wavelength for resonating in the higher frequency band. A circular hole with a radius of r_h is inserted into the patch to further improve the impedance matching characteristics. The ring patch is placed at the outer perimeter of the circular patch and has a width of w_2 and a total length of about one wavelength for the lower frequency band. To provide a wide range of the dual-frequency-band ratio adjustment with CP properties, two output ports of a hybrid chip coupler (XC1400P-03S, Anaren, Inc., East Syracuse, NY, USA), denoted as Port 1 (X_1, Y_1) and Port 2 (X_2, Y_2), are connected to the circular patch using via pins, and the central angle of Port 1 and Port 2 is designed to be about 90° with respect to the patch center. Note that the hybrid chip coupler used in our approach is suitable for exciting the antenna with the equal amplitudes and a phase difference of approximately 90° in the L band (1 GHz ≤ *frequency* ≤ 2 GHz) and is embedded on a printed circuit board (PCB) as a feeding network with coplanar waveguides and a 50-Ω termination chip. The ring patch is then electromagnetically coupled with the circular patch, and the coupling strength is controlled by the gap g. The dual-frequency-band ratio can be adjusted by varying this gap; for example, the dual-frequency-band ratio increases as the gap becomes larger and decreases when the gap has smaller values.

To verify the feasibility of the dual-frequency-band ratio adjustment, the proposed antenna is applied for the GPS L1 and L2 bands, whose dual-frequency-band ratio is 1.28. This ratio can be obtained when the gap distance g is about 0.5 mm, and other values of the detailed design parameters are listed in Table 1.

3. Measurement and analysis

The flexible dual-frequency-band ratio adjustment is demonstrated by fabricating the antenna on the CER10 substrate from Taconic (ε_r = 10.0, tanδ = 0.0035), and the antenna characteristics are measured in a full anechoic chamber. Figure 2(a) shows the fabricated radiating elements, and Figure 2(b) is a photograph of the PCB (FR4, ε_r = 4.4, tanδ = 0.018) with the hybrid chip coupler.

Figure 3 exhibits a comparison of the measured and simulated reflection coefficients as a function of the frequency. To obtain the simulated reflection coefficients, the scattering matrix of the 2-port antenna is computed by using FEKO (Altair, 2015) and is combined with the 4-port network of the hybrid chip coupler in Ansoft Designer (Ansys, Inc., 2013).

Table 1. Optimized values of the proposed antenna.

Parameters	Values (mm)
w_1	11.5
w_2	0.6
g	0.5
r_h	2.0
X_1	4.7
X_2	−6.3
Y_1	6.2
Y_2	4.4
l	55.0
h	14.1

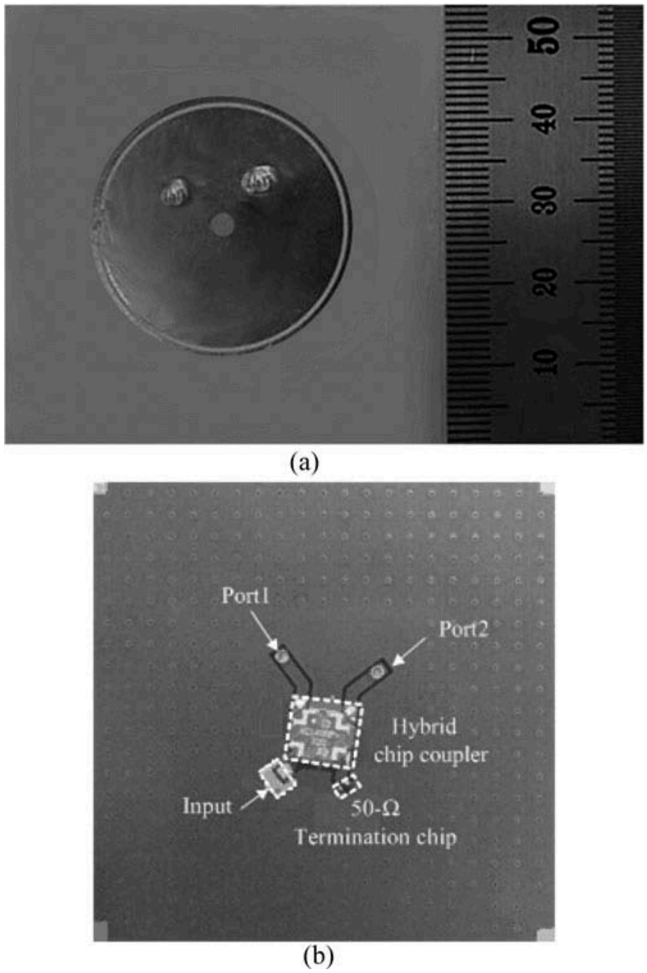

Figure 2. Photograph of the fabricated antenna: (a) top view of the fabricated antenna and (b) printed circuit board with a hybrid chip coupler.

The measured reflection coefficients are –17.9 and –19.6 dB at 1.5 and 1.2 GHz, respectively, which are similar to the simulated reflection coefficients of –16.6 and –20.8 dB.

Figure 4 represents measured bore-sight gains in comparison with the simulation. The dashed line indicates the simulated data, and the measured values obtained in the full anechoic chamber are specified by '+' markers. The measured values are 4.7 and 3.3 dBic at 1.5 and 1.2 GHz, respectively, and the simulated values are 4.0 and 3.2 dBic. The measured dual-frequency-band ratio for the peak gain values is maintained at 1.25, which is similar to the simulated value of 1.28.

Figure 5 indicates a comparison of the AR values in the bore-sight direction. The antenna is circularly polarized with the measured AR values of 0.2 and 1.4 dB at 1.5 and 1.2 GHz, respectively, which are similar to the simulated values of 0.3 and 1.4 dB. As can be observed, the antenna shows a broad 3-dB axial ratio (AR) bandwidth, which allows it to be more flexible for the dual-frequency-band ratio adjustment over a wide range without any serious polarization distortion.

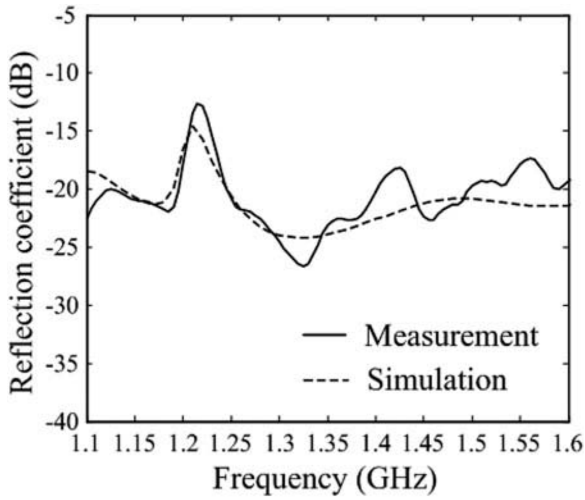

Figure 3. Reflection coefficients of the proposed antenna.

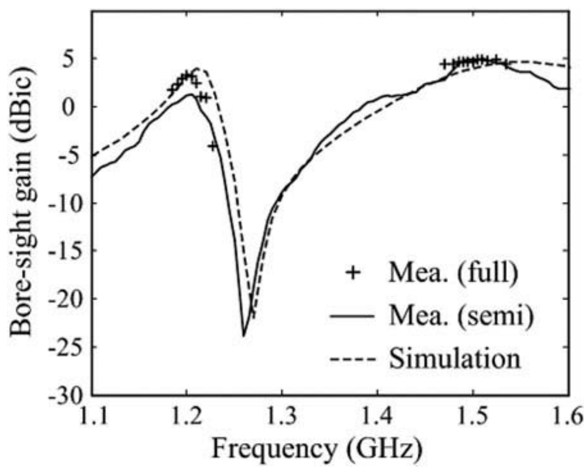

Figure 4. Bore-sight gain of the proposed antenna.

Figure 6 shows comparisons of the measured and simulated radiation patterns at two frequency points. The half-power beamwidths (HPBWs) at 1.5 GHz are 100.8° in the *z*-*x* plane and 99.8° in the *z*-*y* plane. Figures 6(c) and 6(d) indicate patterns in the *z*-*x* and *z*-*y* planes at 1.2 GHz, and their HPBWs are 101.2° and 102.8°, respectively. The measured patterns indicate that the antenna has a wide beam coverage of greater than 90° without any serious gain degradation or pattern distortions in the upper hemisphere.

Figure 7 shows variations of the dual-frequency-band ratio and AR values according to the gap distance *g*. The left vertical axis indicates the dual-frequency-band ratio, which is defined as the lower resonant frequency (f_1) divided by the higher resonant frequency (f_2), and the right vertical axis shows the AR values averaged in the two frequency bands. The gap is varied from 0.2 to 5.6 mm at intervals of 0.6 mm, and the increased value of *g* shifts the higher resonance toward the higher frequency band. As a result, the dual-frequency-

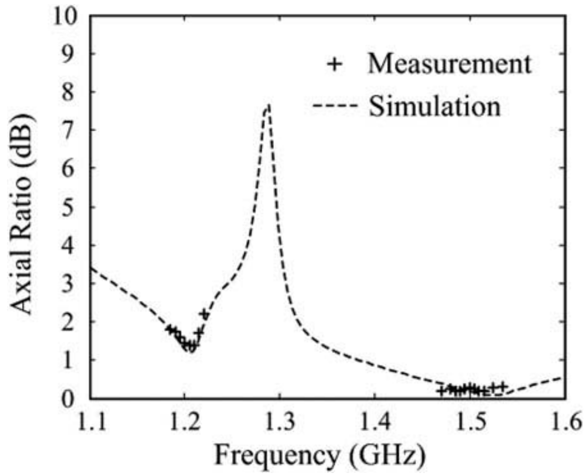

Figure 5. Axial ratio of the proposed antenna.

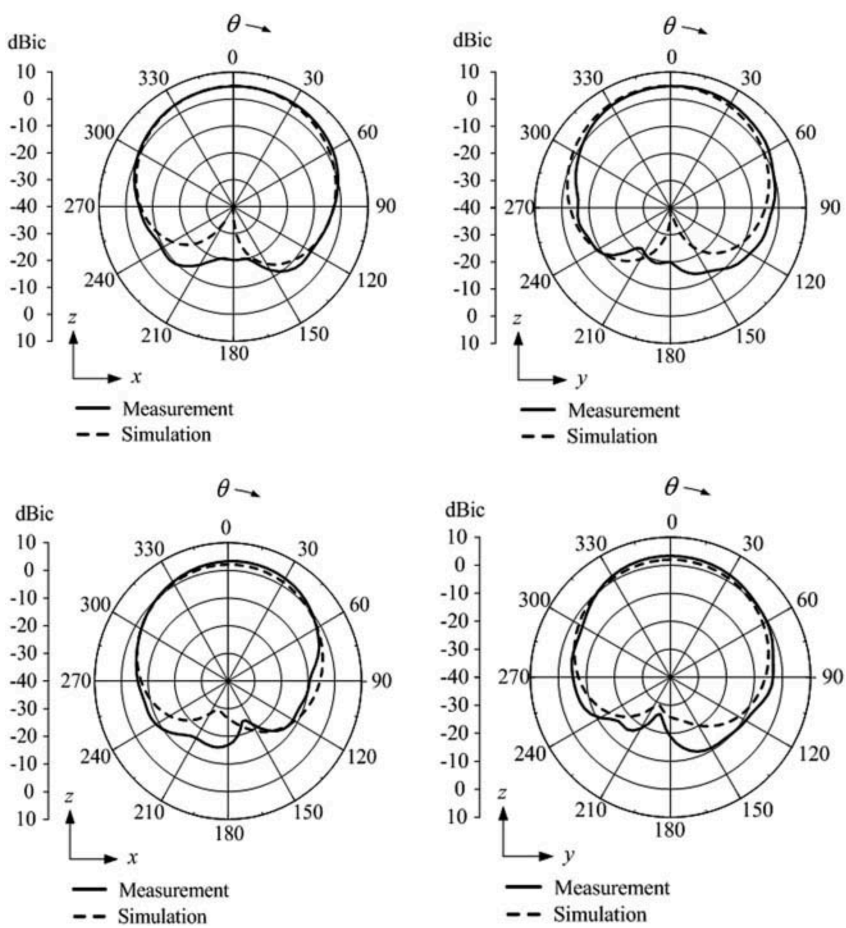

Figure 6. 2D radiation patterns of the proposed antenna: (a) *z-x* plane at 1.5 GHz, (b) *z-y* plane at 1.5 GHz, (c) *z-x* plane at 1.2 GHz, and (d) *z-y* plane at 1.2 GHz.

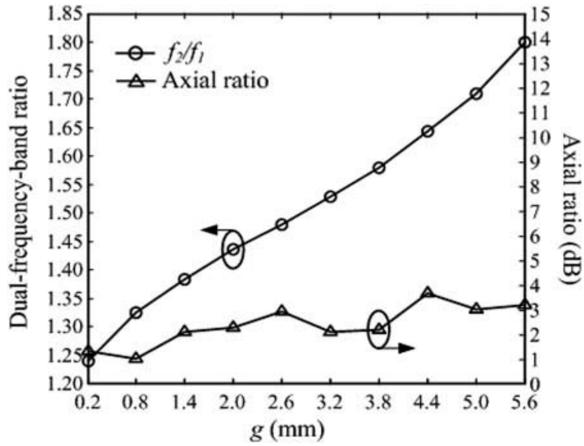

Figure 7. Variations of the frequency ratio and AR according to *g*.

band ratio can be varied from 1.24 to 1.8, with average AR values of less than 3.3 dB in the entire range of the gap distances.

The impedance matching characteristics are also observed by varying the gap distance *g* in the same range, as presented in Figure 8. The solid line with circular markers shows resistance, while the line with triangular markers indicates reactance, which is averaged in the two resonant frequencies. The antenna maintains a resistance of about 50 Ω with almost zero reactance, which results in reflection coefficients of less than −10 dB in the entire range. These results demonstrate that the proposed antenna structure is suitable for adjusting the dual-frequency-band ratio using the single parameter *g* while maintaining the impedance matching and CP characteristics over a wide frequency range.

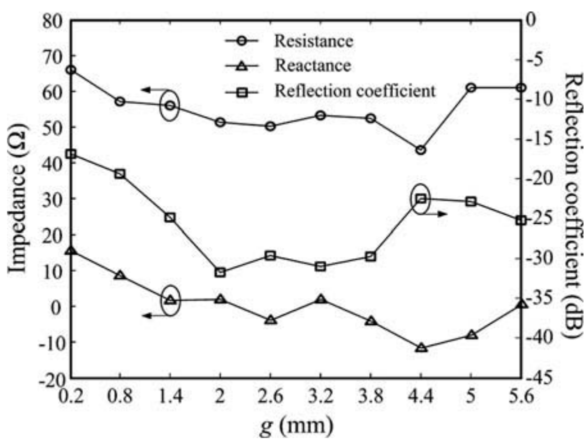

Figure 8. Variations of the input impedance and reflection coefficients according to *g*.

4. Conclusion

The design of a single-layer CP antenna was investigated for a flexible dual-frequency-band ratio adjustment. The proposed antenna consists of an inner circular patch and an outer ring patch, and the gap between the patches was adjusted to vary the dual-frequency-band ratio. The antenna was fabricated to demonstrate the capability of the dual-frequency-band ratio adjustment, and its antenna characteristics were measured in a full anechoic chamber. The antenna showed the bore-sight gains of 4.7 dBic at 1.5 GHz and 3.3 dBic at 1.2 GHz with the measured dual-frequency-band ratio of 1.25. The measured reflection coefficients were −17.9 and −19.6 dB, and the AR values were 0.2 and 1.4 dB in the two frequency bands. The results confirmed that the antenna is suitable for the flexible dual-frequency-band ratio adjustment without the impedance matching and CP distortions.

Funding

This research was supported by the Civil Military Technology Cooperation (CMTC) and the Basic Science Research Program through the National Research Foundation of Korea (NRF) funded by the Ministry of Education (No. 2015R1A6A1A03031833).

References

Abutarboush, H. F., R. Nilavalan, S. W. Cheung, K. M. Nasr, T. Peter, D. Budimir, & H. Al-Raweshidy. 2012. A reconfigurable wideband and multiband antenna using dual-patch elements for compact wireless devices. *IEEE Trans. Antennas Propagat*. 60:36–43.

Altair. 2015. FEKO. Available on-line at https://www.feko.info. Accessed 21 April 2017.

Ansys, Inc. 2013. Ansys Designer v2.2. Available on-line at http://www.ansys.com. Accessed 11 September 2015.

Bao, X. L., & M. J. Ammann. 2007. Dual-frequency circularly-polarized patch antenna with compact size and small frequency ratio. *IEEE Trans. Antennas Propagat*. 55:2104–2107.

Behdad, N., & K. Sarabanni. 2006. Dual-band reconfigurable antenna with a very wide tunability range. *IEEE Trans. Antennas Propagat*. 54:409–416.

Byun, G., H. Choo, & S. Kim. 2015. Design of a dual-band quadrifilar helix antenna using stepped-width arms. *IEEE Trans. Antennas Propagat*. 63:1858–1862.

Byun, G., S. Kim, & H. Choo. 2014. Design of a dual-band GPS antenna using a coupled feeding structure for high isolation in a small array. *Microw. Opt. Technol. Lett*. 56:359–361.

Cai, Y.-M., K. Li, Y.-Z. Yin, & X. Ren. 2015. Dual-band circularly polarized antenna combining slot and microstrip modes for GPS with HIS ground plane. *IEEE Antennas Wireless Propagat. Lett*. 14:1129–1132.

Edimo, M., P. Rigoland, & C. Terret. 1994. Wideband dual polarized aperture-coupled stacked patch antenna array operating in C-band. *Electron. Lett*. 30:1196–1198.

Falade, O. P., Y. Gao, X. Chen, & C. Parini. 2013. Stacked-patch dual-polarized antenna for triple-band handheld terminals. *IEEE Antennas Wirel. Propagat. Lett*. 12:202–205.

Hsieh, W.-T., T.-H. Chang, & J.-F. Kiang. 2012. Dual-band circularly polarized cavity-backed annular slot antenna for GPS Receiver. *IEEE Trans. Antennas Propagat*. 60:2076–2080.

Hu, Z. H., C. T. P. Song, J. Kelly, P. S. Hall, & P. Gardner. 2009. Wide tunable dual-band reconfigurable antenna. *Electron. Lett*. 45:1109–1110.

Hung, C., & T. Chiu. 2015. Dual-band reconfigurable antenna design using slot-line with branch edge. *IEEE Trans. Antennas Propagat*. 63:508–516.

Nasimuddin, Z., N. Chen, & X. Qing. 2010. Dual-band circularly polarized S-shaped slotted patch antenna with a small frequency-ratio. *IEEE Trans. Antennas Propagat*. 58:2112–2115.

Nor, M. Z. M., S. K. A. Rahim, M. I. Sabran, P. J. Soh, & G. A. E. Vandenbosch. 2013. Dual-band, switched-beam, reconfigurable antenna for WLAN applications. *IEEE Antennas Wirel. Propagat. Lett*. 12:1500–1503.

Reddy, G. S., A. Kamma, S. K. Mishra, & J. Mukherjee. 2014. Compact Bluetooth/UWB dual-band planar antenna with quadruple band-notch characteristics. *IEEE Antennas Wirel. Propagat. Lett*. 13:872–875.

Smolders, A. B., R. M. C. Mestrom, A. C. F. Reniers, & M. Geurts. 2013. A shaped aperture dual-frequency circularly polarized microstrip array antenna. *IEEE Antennas Wirel. Propagat. Lett*. 12:120–123.

Ta, S. X., & I. Park. 2014. Multiband-notched UWB antenna using folded slots in the feeding structure. *J. Electromag. Eng. Sci*. 14:31–35.

Zhang, T., W. Hong, Y. Zhang, & K. Wu. 2014. Design and analysis of SIW cavity backed dual-band antennas with a dual-mode triangular-ring slot. *IEEE Trans. Antennas Propagat*. 62:5007–5016.